Supplementary information

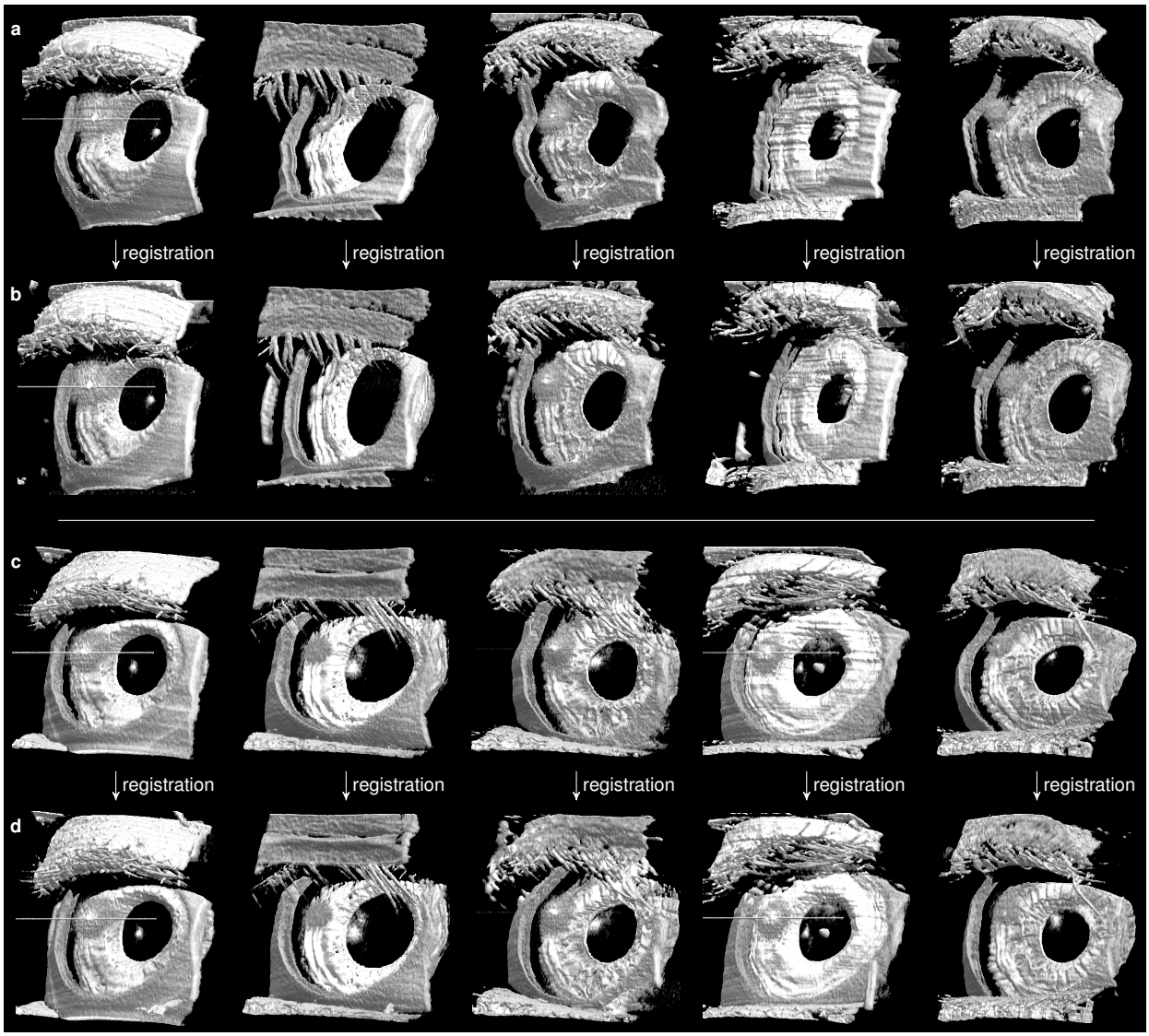

Supplementary Fig. 1 | Side-by-side comparison of registration for anterior volumes. **a**,**c** Paired right (a) and left (c) volumes without registration from 5 different individuals corresponding to Fig. 5a,c which exhibit a combination of lateral and axial motion artifact. The cornea and iris are held within the OCT axial imaging range, however, permitting correction in post-processing. **b**,**d** Registered volumes reproduced from Fig. 5a,c for comparison, which demonstrate removal of residual motion artifact.

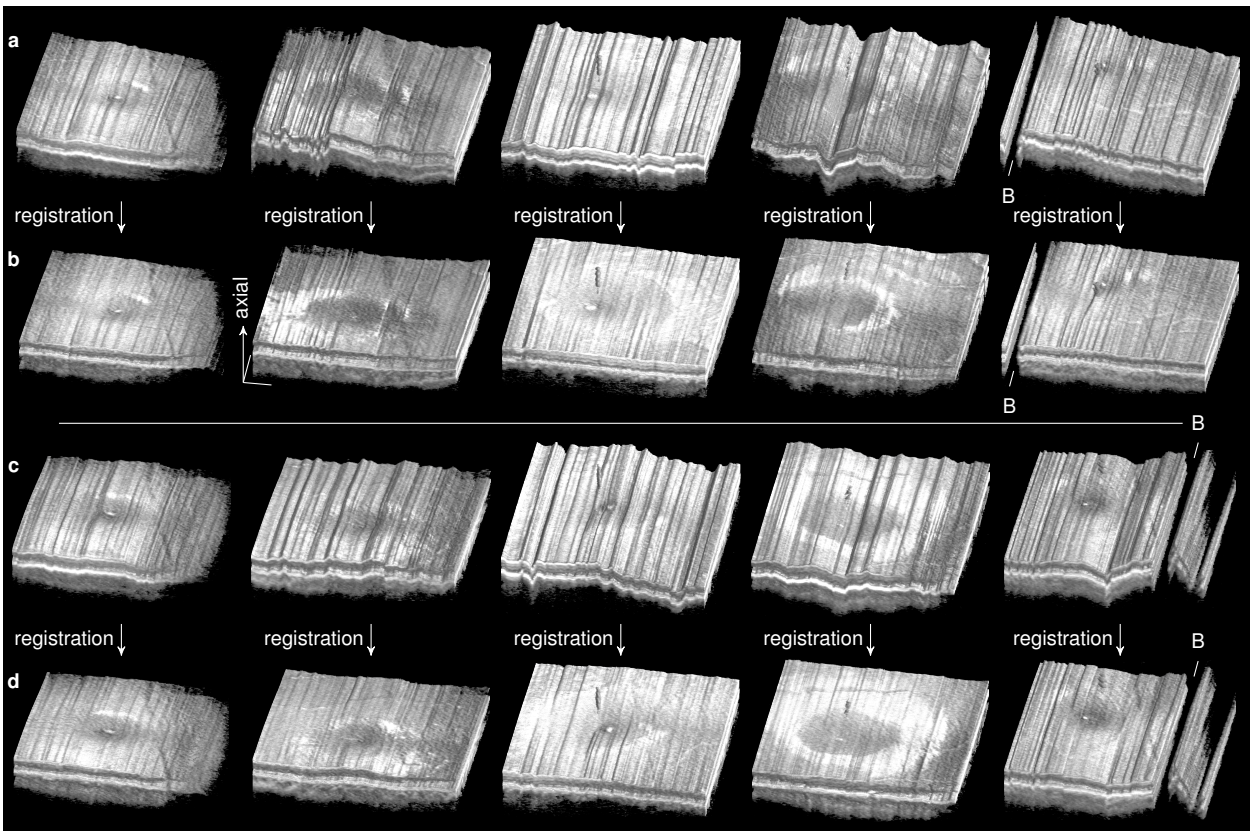

Supplementary Fig. 2 | Side-by-side comparison of registration for retinal volumes. a,**c** Paired right (a) and left (c) volumes without registration from 5 different individuals corresponding to Fig. 6a,c. Volumes are axially stretched by a factor of 2 as in Fig. 6 which accentuates the axial motion artifact. The retina remained within the OCT axial imaging range, except during and shortly after blinks. **b**,**d** Registered volumes reproduced from Fig. 6a,c for comparison, which demonstrate removal of most residual motion artifact. Persistent motion artifact was due to slight tilting of the retina and stretching introduced by scanning while the reference arm was in motion. B, artifact from blink.

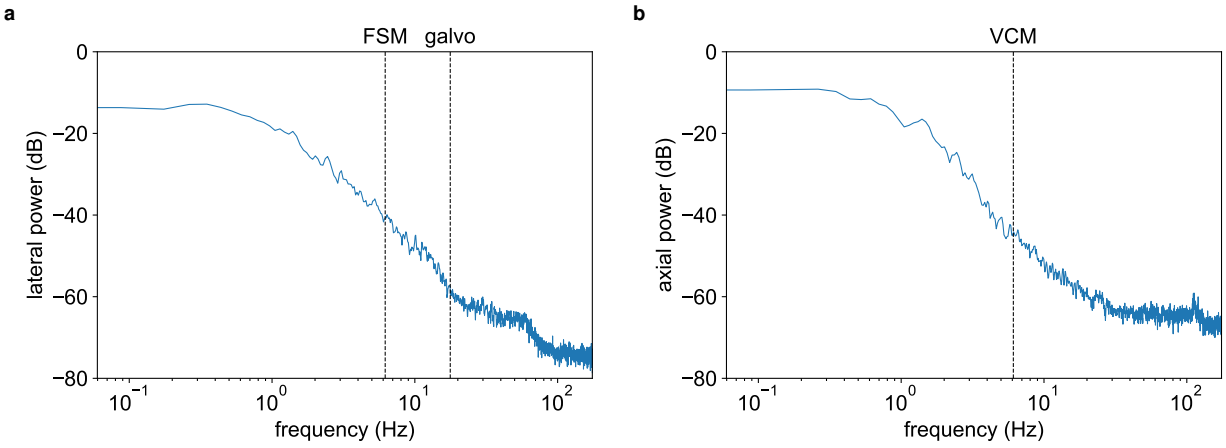

Supplementary Fig. 3 | Pupil alignment error power spectra from all autonomous imaging sessions. a, Mean lateral power spectrum of tracked pupil position relative to the scan head once the robot had achieved gross alignment. The majority of spectral power was concentrated within a frequency range below the theoretical maximum correction frequencies of 6.2 Hz and 17.7 Hz for the FSM and galvanometers, respectively. Gaps in telemetry due to blinks and tracking failures were filled using linear interpolation to enable frequency analysis. **b**, Mean axial power spectrum of tracked pupil position relative to the scan head once the robot had achieved gross alignment. The majority of spectral power was concentrated within a frequency range below theoretical maximum correction frequency of 6.1 Hz for the VCM. Gaps filled as with **a**.

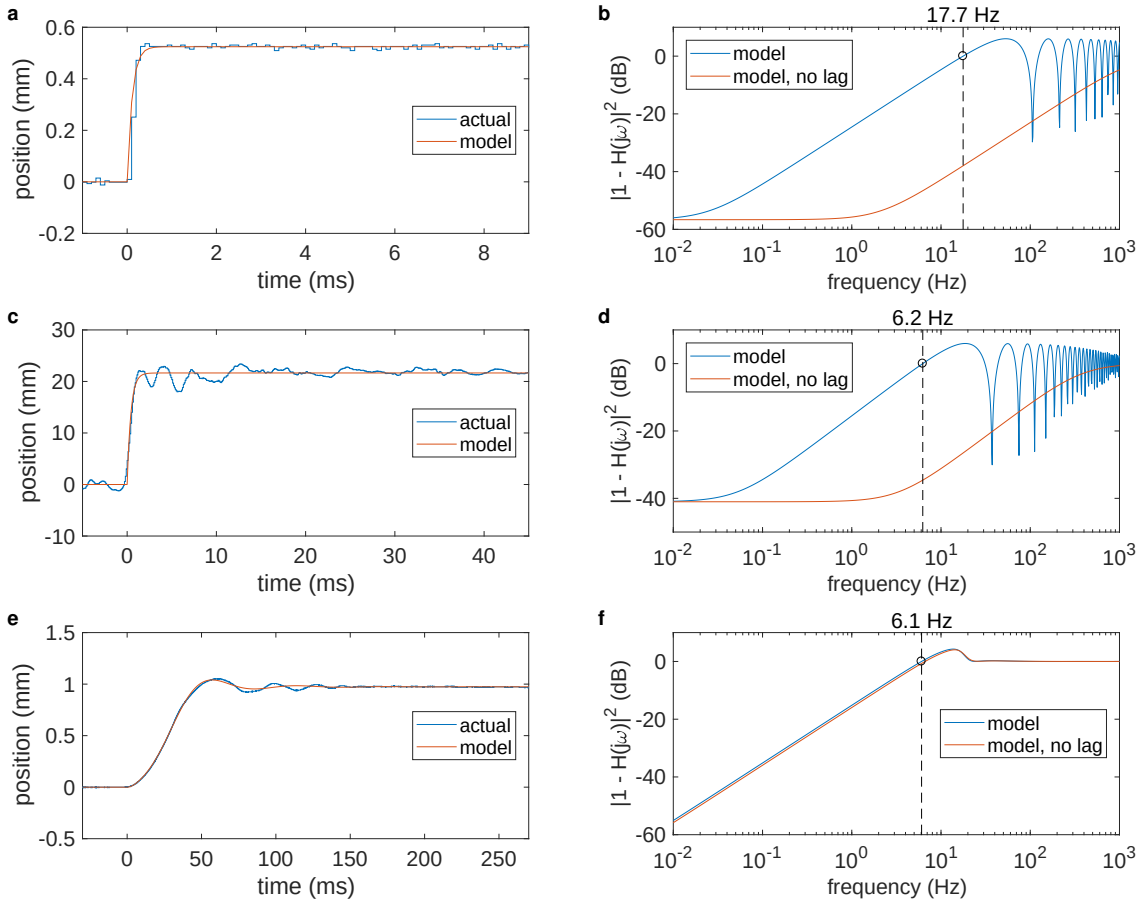

Supplementary Fig. 4 | Step and frequency response modeling for active tracking components. a, Galvanometer experimental step response (blue) and model output (orange). **b**, Model-based frequency response of galvanometer tracking error with (blue) and without (orange) lag, indicating a maximum attenuation frequency of 17.7 Hz. **c**, FSM experimental step response (blue) and model output (orange). **d**, Model-based frequency response of FSM tracking error with (blue) and without (orange) lag, indicating a maximum attenuation frequency of 6.2 Hz. **e**, VCM experimental step response (blue) and model output (orange). **f**, Model-based frequency response of VCM tracking error with (blue) and without (orange) lag, indicating a maximum attenuation frequency of 6.1 Hz.